Radiation hazard evaluation and spatial dose rate mapping in mineralized region of Siwaliks: A case study from Una, Kangra and Hamirpur distt, Himachal Pradesh, India.

Pragya Pandit*[a], Dibakar Ghosh [a]

[a]*Atomic Minerals Directorate for Exploration and Research, New Delhi, India*

Abstract

The following work is a part of wider uranium prospecting programme of the Atomic Mineral Directorate for Exploration and Research (AMD) for mapping radioactive anomalies in mineralized regions of Siwalik, Himachal Pradesh. This study reports the analysis of average activity concentration, potential radiological hazards; radium equivalent activity (Ra_{eq}), external hazard index (H_{ex}), internal hazard index (H_{in}) and excess cancer life time risk (ECLR) calculated due to naturally occurring radioactive materials (NORM); Radium (^{226}Ra), Thorium (^{232}Th) and Potassium (^{40}K) in uranium mineralized zone of Siwaliks for health risk assessment. The geometric mean value of calculated indoor and outdoor annual effective dose in the Una, Hamirpur and Kangra region are 0.88 and 0.22; 1.77 and 0.44; 1.86 and 0.46 $mSvy^{-1}$ respectively. The average air absorbed dose rate were measured to be 118 $nGyh^{-1}$ in Una, 163 $nGyh^{-1}$ in Hamirpur and 135 $nGyh^{-1}$ in Kangra district respectively. Correlation study indicated good correlation of the measured gamma dose rate and the estimated gamma dose rate with a correlation coefficient of (R^2 =0.62). Our data provides important information on the radiation risk and spatial variability of the natural terrestrial gamma radiation in the Siwalik region.

Keywords:, Radiological hazard indices, Radioactivity, Gamma radiation survey, Gamma spectrometry

** Corresponding author. Tel.: +91 11 25584443*
** E-mail address: pragyapandit.amd@gov.in*

1. Introduction

Living organisms on the earth have been receiving the radiation exposure continuously from cosmic rays, terrestrial radionuclides (^{235}U, ^{238}U, ^{232}Th and ^{40}K), cosmogenic nuclides (^{7}Be, ^{14}C, ^{18}F, ^{22}Na etc.) and anthropogenic radionuclides (^{137}Cs) (UNSCEAR 1993). The total annual effective dose from the natural radiation sources is 2.3 $mSvy^{-1}$ in India as compared to the global contribution of 2.4 $mSvy^{-1}$ (UNSCEAR 1982; UNSCEAR 2000; UNSCEAR 2008; UNSCEAR 2000b). In India, natural sources that account for exposure to environmental radiation include cosmic radiation (15.44%), terrestrial radiation (internal and external)(30.18%), ^{222}Rn and ^{220}Rn inhalation (53.72%) and cosmogenic nuclide (inhalation) (0.65%). The worldwide average annual effective dose equivalent due to terrestrial gamma radiation is 0.48mSv. Large evidences are present that support the study that radiation exposure above a certain threshold level could induce heredity disorders, leukemia and cancers of different organs such as lungs, kidney (Editing et. al. 1982; Flodin et. al.1990; Murrihead et al. 1990). Significantly high radiation doses have been received by human population residing in regions of high atomic mineral occurrences. In the previous years, many studies for estimating the natural radiation hazard indices (Ra_{eq}, H_{ex}, H_{in} and ECLR); indoor and outdoor gamma dose rate (γ) have been conducted in places of atomic mineral occurrences (Bhattacharya et al. 2018; Srinivas et al. 2016; Maharana et al. 2010; Karunakara et al. 2014; Kadam et al. 2014; Patra et al. 2013) and that from high level natural radiation areas (HLNRA) (Ghiasinejad et. al. 2002 and 2004; Mohanty et al. 2004; Kardan et al. 2017; Shetty et al. 2010; Sunta 1993).

Uranium exploration is the prime mandate of AMD and there are six prime investigation areas. Airborne (AGRS) and ground based radiometric survey is carried out in the preliminary stages of uranium investigation for delineating and identifying radiation anomalies in uranium prospecting and for baseline environmental survey (Grasty and Lamairre 2014). Since these are mineralized regions with high concentration of primordial activities hence there is high probability of large radiation doses being imparted to the local population. This requires monitoring of gamma dose rate and radionuclide concentration for health risk assessment in the mineralized and in the background region. A detailed investigation on radiation monitoring has already been conducted on various high atomic mineral occurrences sites of Gogi, Dharmapuri and Jaduguda. Srinivass et al. has revealed average dose of 186 $nGyh^{-1}$ in Chitrial, 130 $nGyh^{-1}$ in Lambapur-Pedaguutu and 63 $nGyh^{-1}$ in koppunura in uranium mineralized region of Gogi. The average annual effective dose rate in the Dharmapuri shear zone was estimated by Bhattacharya et al. and was observed to be above the recommended limit of 1 $msvy^{-1}$. Siwaliks region is known for hosting sandstone type of uranium deposits. Exploratory mining carried out at Andalada in Siwaliks have delineated six discontinuous ore lenses over 330 x 100 m with thickness of 0.98 to 2.2m. A total of 3058 tonnes of ore with 0.02-0.045 % eU_3O_8 in first level containing 2.32 tonnes of U_3O_8 was proved. Hence a foot based radiation survey and soil sampling of grab samples is being carried out to map the dose rate in this region for health risk assessment.

Recently spatial modeling has been utilized to visually characterize the transport behavior of radionuclides (akoczan et al. 2018; Shetty et al; Cavalcante et al 2011; Al Azami et al. 2017; Szegvary 2007; Harun et al. 2018). Radiometric maps are drawn to interpret geophysical activity and radionuclide migration. Previous literature on radiological parameters study has only demonstrated the radionuclide concentration and hazard parameter study in this region; however none of the above studies has demonstrated the spatial variability of radionuclides. Our report is divided into two parts. We have tried to determine the background radiation in the uranium mineralized region of Una, Hamirpur and kangra and evaluate radiation hazard by evaluating different radiological indices and visually characterize the migratory behavior of radionuclides using spatial modeling. The obtained data may be the baseline for future research, environmental monitoring and epidemiological studies in the studied area.

2. Geology

The study area (Siwalik) is in northern part of India and covers an area of 2500 sq km. The basin, comprising the Siwalik sediments, extends over >2500 km from Potwar plateau, Pakistan in NW to Arunachal Pradesh. The study area extended from 31º37’30” N to 32º9’0” N latitudes and 75°51’0”E to 76°33’0” E longitude. The Siwalik sediments considered as favourable host for epigenetic sandstone type of uranium mineralization due to their sedimentological character, provenance and depositional environment. The rocks of Siwalik group are divided into upper, middle and lower siwalik groups. The area of present investigation, ie. Rajpura-Nari-Jawar-Parah area falls within the Kangra sub-basin within the middle and upper siwalik the northern limit of which is defined by the Main Boundary Thrust (MBT) whereas the southern margin is bounded by Soan and Barsar thrust. The geological map and location map of Siwaliks is shown in the **Fig 1(a) and Fig 1(b)**. The Siwalik sediments are deposited along the number of foreland basins of Himalaya. The Siwaik Group (Middle Miocene to Pleistocene) represents ca.6000m thick molasse deposit. These sediments have been traditionally been divided into Lower, Middle and Upper Siwalik. Lower Siwalik is a distinct assemblage of fine sandstone- mudstone, whereas sandstone-conglomerate package represents Middle Siwalik and Upper Siwalik comprises of gravel/boulder bed with minor sandstone. Contacts between the formations are gradual and conglomerate dominance increase towards top. Kangra subbasin possess the thickest deposits of Siwalik rocks and the most promising according to the uranium mineralisation point of view (Kaul et al. 1979; Kaul et al.1993; Bala et al. 2014), Occurrences of number of radioactivity

in this basin attracted this study of radiation dose in the area. Investigating area of Rajpura-Nari-Jawar-Parah area falls within the Soan &Barsar thrust and here radioactivity is hosted by Upper Part of Middle Siwalik pebbly sandstone-conglomerate. And the Loarkhar-Sibbal area falls in Barsar &Soan thrust; here radioactivity is hosted by Middle Siwalik pebbly sandstone-conglomerate. Uranium mostly occur as adsorbed phase with the mud clast, coaly matter, clay minerals. **Table 1.** describes the sampling areas of Himachal Pradesh.

3. Materials and Methodology

Based on the activity of the radionuclides (> 3 Bg) and geological background, a total of 218 grab samples were collected from the 33 different locations of Una, Hamirpur and Kangra district, Himachal Pradesh, India during the period of 2016-2017. These sample locations were numbered as S_1 to S_{33}. The sampling area, sampling sites, geographical location, dose rate measured and geological parameters are listed in **Table 2**. In order to collect the natural soil, the soil samples weighing about 250 gm have been collected at a depth of 75 cm from the surface. Distance between each location was 1 km. The corresponding latitudes and longitudes were noted using a GPS make (Global positioning system). The sample were homogenized, pulverized and then sieved through -150 mesh. The samples were then dried in oven for about 24 hours. Quantitative determination of ^{226}Ra, ^{232}Th and ^{40}K was performed by Gamma ray spectrometric system using NaI(Tl) gamma detector of size 5" × 4" coupled with photomultiplier tube and a DSP based 2K MCA system. Spatial distribution modeling analysis using ARCMAP GIS (Geographical Information Software) has been adopted for modeling of terrestrial radionuclide activity (in $BqKg^{-1}$) due to the distribution of gamma dose rate, Ra_{eq} (in ppm), Thorium (in ppm) and K (in %). Statistical analysis was performed with SPSS 20 (Statistical Program for Social Science). The geoelemental values are presented by arithmetic mean (AM), geometric mean (GM), and range (R). The dispersion in the parameters are expressed by standard deviation (SD), Interquartile range (IQR) and median absolute deviation (MAD). The outliers (cases with standardized residual greater than ±3 standard deviations) found in the data were removed for calculation of radiation hazard indices. The asymmetry and tailness of the distribution is indicated by the skewness (Sk) and kurtosis (K) of the data. Further the data have been tested for normality (Kolmogorov-Smirnov). The frequency distribution indicating the normality of the radioelemental data is visualized by Q-Q (Quantile -Quantile) plots. Pearson correlation analysis, cluster analysis was performed to find correlation between radiological parameters. All tests were performed at 95% confidence interval and value of $p<0.05$ were considered statistically significant.

3.1 Estimation of ^{226}Ra, ^{40}K and ^{232}Th concentration by gamma ray spectrometry

The activity concentration of ^{226}Ra, ^{232}Th and ^{40}K were determined by NaI(Tl) detector. The detector has an active volume of 1286.38 cm^3, a resolution of 9.5% and an efficiency of 14.5 % at 662 keV. The detector was surrounded by lead shield with dimensions of 2"x 4"x8" to reduce background. The detector was calibrated w.r.t the 667 KeV peak of ^{137}Cs and 1.17 and 1.33 MeV of ^{60}Co. The spectral analysis was done with the help of computer software WinTMCA. The activity concentration of ^{226}Ra was obtained by analyzing the gamma ray line of ^{214}Bi (1.76 MeV) (Bikit et al. 2004). ^{232}Th activity concentration was measured by analyzing the gamma ray peak of ^{208}Tl (2.42 MeV) whereas, the concentration of ^{40}K was determined by analyzing the photo peak of 1.46 MeV(IAEA 2003).The activity concentrations of these soil samples were quantified with respect to the standard sources of natural ^{238}U, ^{232}Th and ^{40}K by using Eqs.(1-4) . Details using the methodology are described using IAEA tech doc 1363. The samples were counted for a time of 500s and two replicate analysis were carried out to keep the error within ±2σ. The concentrations of ^{226}Ra$\left(C_{Ra}(BqKg^{-1})\right)$, ^{232}Th ($C_{Th}(BqKg^{-1})$) and ^{40} K$\left(C_K(BqKg^{-1})\right)$ were estimated by

$$\sum_{i=1}^{3} n_i = \sum_{i=1}^{3}\sum_{j=1}^{3} S_{ij} C_j \qquad (1)$$

$C_{j=1,2,3}$ = concentration of the j^{th} element (% K, U in ppm, Th in ppm),

n_i = gamma rate of counts in the K, U and Th channel,

S_{ij} = are the sensitivityof the gamma ray detector in a given window expressed as net rate of count per unit concentration,

The stripping ratio α, β, γ related to the concentration as

$$Th_n = Th_g – aU_n \qquad (2)$$

$$U_n = U_g - \alpha Th_n \qquad (3)$$

$$K_n = K_g – \beta Th_n - \gamma U_n \qquad (4)$$

are given by

$$\alpha = \frac{S_2 Th}{S_3 Th}, \qquad \beta = \frac{S_1 Th}{S_3 Th}, \qquad \gamma = \frac{S_1 U}{S_2 U}, \qquad a = \frac{S_3 U}{S_2 U}, \qquad b = \frac{S_3 K}{S_1 K}$$

The minimum detection limit of ^{226}Ra, ^{232}Th and ^{40}K are 2.65 Bq kg^{-1}, 3.53 Bq kg^{-1} and 15.8 Bq kg^{-1}respectively.

3.2 Estimation of Radiological Hazard indices

The radiological Hazard indices Radium equivalent(Ra_{eq}), Air absorbed dose rate, D(nGyh^{-1}) , annual effective dose equivalent, AEDE (indoor and outdoor) (mSvy^{-1}), Hazard Indices (External and Internal) (H_{ex} and H_{in}), Gamma Index(I_γ), Excess cancer lifetime risk (ECLR) have been calculated using the conversion factors given by UNSCEAR and other agencies as discussed in results and discussion part of the manuscript (UNSCEAR, 1993; UNSCEAR, 1982; UNSCEAR, 1988; Beretka and Mathew, 1985).

3.3 Geostatistical Interpolation

Spatial distribution modeling was performed using IDW (Inverse Distance weighted) algorithm on Arc map GIS (Geographical Information System) 10.3 software. The Inverse Distance weighing (IDW) interpolation technique is based on the assumption that the nearby values contribute more to the interpolated values than the distant observation (Watson and Philip 1985). The IDW interpolation uses the weight function w_i given by equation (5) (Mitas and Mitasova, 1999).

$$w_i = \frac{h_i^{(-p)}}{\sum_{j=0}^{j=n} h_j(p)} \qquad (5)$$

Where p is an arbitrarily positive number called the power parameter and h_j are the distances from the dispersion points to the interpolation points, given by

$$h_i = \sqrt{(x - x_i)^2 + (y - y_i)^2} \qquad (6)$$

Where x, y are the coordinates of the interpolation points and x_i and y_i are the coordinates of each dispersion points. There are 190 sampling points that are measured at different locations of Una, Hamirpur and Kangra districts of Himachal Pradesh. The survey points were transferred to a basemap to create geodatabase.

4. Results and Discussion

4.1 Soil Radioactivity (^{226}Ra, ^{232}Th and ^{40}K) :

The descriptive statistics of geo-elemental radioactivity concentration of ^{226}Ra, ^{232}Th and ^{40}K in Una, Hamirpur and Kangra region are given in **Table 3**. The concentration of ^{226}Ra, ^{232}Th and ^{40}K in Una region was varied from 8 Bq kg^{-1} to 3593 Bq kg^{-1}, 21 Bq kg^{-1} to 370 Bq kg^{-1} and 217 Bq kg^{-1} to 7130 Bq kg^{-1} with mean value of 433 Bq kg^{-1}, 66 Bq kg^{-1} and 764 Bq kg^{-1} respectively. **Fig 2 – 5** revealed the graphical demonstration of activity concentration of ^{226}Ra, ^{232}Th and ^{40}K in the studied region. **Fig 2** revealed the huge variation of ^{226}Ra activity in Dadoh west and Polion east of Una region. The grey sandstone rock type without any mudstone is responsible for low uranium content in Dadoh west. However, Polion east has medium to fine sandstone bedrock with slit laminae and matrix supported conglomerate mudstone that causes ideal uranium adsorption. In Hamirpur region, the concentration of three radionuclides (^{226}Ra, ^{232}Th and ^{40}K) varied from 43 Bq kg^{-1} to 3603 Bq kg^{-1}, 21 Bq kg^{-1} to 102 Bq kg^{-1} and 62 Bq kg^{-1} to 2449 Bq kg^{-1} with mean value of 818 Bq kg^{-1}, 65 Bq kg^{-1} and 754 Bq kg^{-1} respectively. In the middle Siwalik region (brown colored coarse grained pebbly sandstone), a very high ^{226}Ra concentration (6833 Bq kg^{-1}) was observed at S_{21} sampling site (Loharkar old) as it lies between Jwalamukhi and Barsar thrust that exposes of transition zone of middle and upper Siwalik as shown in **Fig 3**. The sandstone type of uranium mineralization is associated with mudstone bed (highly alkaline depositional environment) and hosts radionuclides in this area.

The activity concentration of ^{226}Ra, ^{232}Th and ^{40}K in Kangra region varied from 122 Bq kg^{-1} to 2009 Bq kg^{-1}, 41 Bq kg^{-1} to 100 Bq kg^{-1} and 558 Bq kg^{-1} to 2449 Bq kg^{-1} with mean value of 789 Bq kg^{-1}, 67 Bq kg^{-1} and 815 Bq kg^{-1} respectively. A high ^{226}Ra activity concentration (1933 BqKg-1) was observed in Dhuli Bhatawan area (S_{25}) due to region bounded by Soan thrust in the west and Barsar thrust in the east with yellowish brown oxidized sandstone and whitish grey homogeneous sandstone rock type. No significant variation was observed in the activity concentration of ^{232}Th in studied region (**Table 3**). The overall mean activity concentration of ^{40}K was also observed to be homogeneous in the studied region. The ^{40}K concentration was higher due to the excessive feldspar in the Siwalik area. The Quartz and Feldspar (plagiocase and K feldspar) are uniformly distributed in the rocks and gradually elevate the ^{40}K concentration in this region. In this region, ^{226}Ra and ^{40}K determined almost uniform pattern with increase concentration towards Dhuli Bhatawan (south) and decrease along Dhanota Nala (east) as shown in **Fig 4**. ^{232}Th also has same distribution with high concentration along Manawala and low towards Dhuli Bhatawan. The Dhuli Bhatawan region consist grey sandstone and feldspar. Petrological study revealed that radioactive samples of Gamir Khad and Dhul area are ferruginous silty shale to shaly silt stone and composed of silt size clasts of quartz and feldspar admixed with ferruginous clay matrix. **Fig 5.** shows the radionuclide concentration in the Siwalik region.

The Q -Q (Quantile -Quantile) probability plots have been used to confirm the statistical distribution of data around their mean. **Fig 6(a)- 6(c)** demonstrates the normal and log-transformed Q-Q plots of ^{226}Ra, ^{232}Th and ^{40}K activity concentration in Una, Hamirpur and Kangra region. Q-Q plots are frequency distribution curves indicating the normality of a given statistical data. The mean values of ^{226}Ra, ^{232}Th and ^{40}K were greater than their median that indicating non normal distribution. Positively skewed frequency distribution deviating from normality was observed for ^{226}Ra (Sk=2.48, 1.96, 0.82; Ƙ=6.10, 5.08, -0.37), ^{232}Th (Sk=5.71, 0.30, 0.49;

K=47.85, -0.25, -1.02) and ^{40}K (Sk=9.65, 3.09, 4.43; K=105.31, 18.80, 22.07) activity concentration in Una, Hamirpur and Kangra and represent the general trend observed for naturally occurring radionuclides as given in **Table 3**. (Shacklette and Boerngen 1984). The ratio of mean value of ^{226}Ra to ^{232}Th was 6.5 for Una region, 12.5 for Kangra region and 11.8 for Hamirpur region. This activity ratio is due to uranium mineralization in this area. The samples were collected from depth between 75 cm and 1 m and hence the mineralization is present at shallow regions. Further, high disequilibrium factor (^{238}U/^{226}Ra) suggests that the process of uranium mineralization is still under dynamic state and uranium is constantly being moved from clay oxidizing zone and getting precipitated with enrichment in the reduced zone.

The highest concentration of ^{226}Ra is found in sites S_4, S_{15-30}, and that of ^{40}K in S_{1-14}, S_{31-33} (**Fig 5**). Statistically significant difference is observed between the values of ^{226}Ra, ^{232}Th and ^{40}K reported in this paper and the values reported earlier by A. Rani and S. Singh (2005) (57.34 Bq kg^{-1}, 82.22 Bq kg^{-1} and 137.78 Bq kg^{-1}) and Bala et al. in areas of Himachal Pradesh. The values reported are higher for ^{226}Ra (681.94 Bq kg^{-1}) and ^{40}K (766.39 Bq kg^{-1}) and lower for ^{232}Th (66.81 Bq kg^{-1}). The world average concentration of ^{226}Ra, ^{232}Th and ^{40}K are 32 Bq kg^{-1}, 45 Bq kg^{-1} and 412 Bq kg^{-1} (UNSCEAR, 2008). A comparison of average activity concentration of natural radionuclide (^{226}Ra, ^{232}Th and ^{40}K) in soil samples (in Bq kg^{-1}) from high radiation areas of India and world is shown in Table 4. This is due to the fact that the samples are collected from highly mineralized uraniferous zone having high ore grade U concentration (≈ 3000 ppm) and are not representative of the all considered sample regions.

Data was found to be non normally distributed hence, Non parametric correlation test Kendal tau and Spearman rho was performed to find the interrelation between the natural radionuclide and calculate radiological hazard parameters. Cohen's standard has been used to evaluate the correlation coefficient and to determine the strength of relationship or the effect size. Correlation coefficient between $0.1<x<0.29$ represents a small association, coefficients between $0.30<x<0.49$ represents a medium association and $x>0.50$ represents a large association. ^{226}Ra was having a small and positive correlation with ^{232}Th ($r = 0.152$, $p = 0.042$). Since $p<0.05$, hence correlation was statistically significant. In case of ^{226}Ra and ^{40}K ($r=0.004$, $p=0.963$). Similarly in ^{40}K and ^{232}Th ($r=0.013$, $p=0.441$). This implies that ^{40}K has different geochemical origin when compared to ^{226}Ra and ^{232}Th.The results are in agreement with those observed in Singhbhum shear zone (Chakraborty et al. 2009).

Factor analysis was performed to analyze the differences in the variation of the radionuclides. Dimension reduction (EFA) was performed and it was found that KMO test was significant i.e. more than 0.6. It entails sample adequacy and to check Bartlett's test of sphericity. Further $\chi^2=10967.46$ was found significant at $p<0.05$. Communality matrix indicated that ^{226}Ra concentration, ^{40}K concentration, Ra_{eq}, D(nGyh^{-1}), AEDE, H_{ex} and H_{in} and representative γ have similar extraction opposite from ^{232}Th and ^{40}K. The eigen values were coming out to be 1 upto two component level which is also verified through rotated component matrix where component 1 includes ^{226}Ra concentration, Ra_{eq}, D(nGyh^{-1}), AEDE, H_{ex} and H_{in} which implied that ^{226}Ra concentration can explain all radiological hazards independently.

4.2 Radium Equivalent(Ra_{eq}):

Radium Equivalent activity Ra_{eq} is a common radiological hazard index to assess the radiation hazards due to non uniform activity distribution of ^{226}Ra, ^{232}Th and ^{40}K in the soil samples. Ra_{eq} is estimated using the following relation (Beretka and Mathew, 1985; Orgun et al., 2007)

$$Ra_{eq} = C_{Ra} + 1.43C_{Th} + 0.07C_K \qquad (7)$$

whereC_{Ra}, C_{Th} and C_K are the concentration of ^{226}Ra, ^{232}Th and ^{40}K. It is assumed that the same gamma dose rate has been produced by 370 Bq kg^{-1} of ^{238}U, 259 Bq kg^{-1} of ^{232}Th and 4810 Bq kg^{-1} of ^{40}K.

The statistical parameters of Ra_{eq} measurement are given in **Table 3.** The arithmetic mean of Ra_{eq} in Una, Hamirpur and Kangra region was observed to be 581.3, 964.0 and 941.6 Bq kg^{-1}. These values are higher than the maximum permissible value of 370 Bq kg^{-1} as recommended by Organization for Economic Cooperation and Development (OECD 1979). This high Ra_{eq} is due to high mineralization in the localized region.

4.3 Air absorbed dose rate in air (D ($\boldsymbol{nGyh^{-1}}$):

For health risk assessment, the absorbed dose rate are calculated from the activity concentration of ^{226}Ra, ^{232}Th and ^{40}K at a height of about 1 m above the ground using the dose conversion coefficient of 0.461, 0.623 and 0.0414 nGyh^{-1}Bq^{-1}kg^{-1} respectively as given in **Eq. (3)** (Saito and Jacob, 1995). Secular equilibrium has been assumed in between ^{238}U and ^{226}Ra so that the activity concentration of uranium is assumed to be similar to that of radium.

$$D(nGyh^{-1}) = 0.461C_{Ra} + 0.623C_{Th} + 0.0414C_K \qquad (8)$$

The mean, median, std. deviation of the absorbed dose rate has been calculated from the activity concentration of ^{226}Ra, ^{232}Th and ^{40}K for the different areas of Una, Hamirpur and Kangra has been given in Table 3. The absorbed dose rate in the Una, Hamirpur and Kangra region is obtained in the range from 57.6 to 1722 nGy h^{-1}, 87.9 to 1741.3 nGy h^{-1} and 135.2 to 985.6 nGy h^{-1}respectively. The high absorbed dose rate $(nGyh^{-1})$ was observed at DB-16-17\2 (1266.51) and DB-16-17\3 (1741.33) in Kangra region due to secondary uranium minerals. The mean value in the Una, Hamirpur and Kangra region were 272.5, 448.9 and 407.47 nGy^{-1}.

Table a : Comparison of dose contribution due to ^{226}Ra, ^{232}Th and ^{40}K in these respective regions with world average

Places	**% dose contribution due to ^{226}Ra**	**% dose contribution due to ^{232}Th**	**% dose contribution due to ^{40}K**
Una	73.23	15.15	11.06
Hamirpur	84.02	9.02	6.95
Kangra	81.72	10.14	8.13
World Average	25	40	35

Table a depicts the comparative dose due to the relative contribution of ^{226}Ra, ^{232}Th and ^{40}K in the region of Una, Hamirpur and Kangra when compared to the natural region (UNSCEAR 2000). The average value of absorbed dose rate was found to be four times higher than the Indian average value (90 nGyh^{-1} in the range from 27-3051 nGyh^{-1}) and global average value (59 nGy h^{-1} in the range from 18-93 nGyh^{-1}) as reported by UNSCEAR (UNSCEAR, 2007). Similar results of D(nGyh^{-1}) has been obtained by Taru et al.(2018) in higher atomic mineral occurrences of Dharmapuri Shear zone in Tamil Nadu, India.

Fig 7 revealed the box-plot of ^{226}Ra, ^{40}K and ^{232}Th in three regions.

4.4 Annual Effective Dose Equivalent (AEDE):

The AEDE ($mSvy^{-1}$) has been calculated from absorbed dose rate, D ($nGyh^{-1}$) in the studied area using the conversion factor (0.7 $SvGy^{-1}$) and occupancy factor (80%) and (20%) for indoor and outdoor occupancy as discussed by UNSCEAR(UNSCEAR, 2007; UNSCEAR, 2008). The mean, median, geometric mean and standard deviation of the indoor and outdoor AEDE ($mSvy^{-1}$) has been given in Table: 1. The AEDE ($mSvy^{-1}$) is determined using **Eqs. (9) and (10)**.

$$AEDE(Indoor)(mSvy^{-1}) = D(nGyh^{-1}) \times 8760h \times 0.8 \times 0.7(SvGy^{-1}) \quad (9)$$

$$AEDE(Outdoor)(mSvy^{-1}) = D(nGyh^{-1}) \times 8760h \times 0.2 \times 0.7(SvGy^{-1}) \quad (10)$$

The minimum and maximum indoor AEDE ($mSvy^{-1}$) in the Una region were 0.26 and 8.45, and the outdoor AEDE were 0.06 and 2.11 with the average indoor and outdoor values of 1.33and 0.33 $mSvy^{-1}$ respectively. The AEDE ($mSvy^{-1}$) at sampling points PLN-3/11, PLN-3/10 and PLN-3/9 were 31.31, 11.84 and 11.6 respectively, has exceeded the world average due to localized ^{238}U content. In Hamirpur the indoor and outdoor AEDE ($mSvy^{-1}$) has ranged from 0.43 to 8.54 and 0.11 to 2.14 respectively. The mean indoor and outdoor AEDE values were 2.21 and 0.55 $mSvy^{-1}$. The anomalous AEDE indoor (15.8) and outdoor (3.95) $mSvy^{-1}$ was obtained at LRK 16-17/3 and removed as an outlier. The corresponding indoor and outdoor AEDE ($mSvy^{-1}$) of Kangra region varied from 0.66 to 4.83 and 0.17 to 1.21 respectively and the average values were 2.15 and 0.53. The world average indoor and outdoor AEDE ($mSvy^{-1}$) from terrestrial radionuclides is 0.41 and 0.07 $mSvy^{-1}$ (UNSCEAR, 2000). The dose level in India, except HBA (high background radiation area) in the states of Kerala and Tamil Nadu are found to be 0.44± 0.13 $mSvy^{-1}$ (Karunakaraetal. 2014). The estimated AEDE is in agreement with the findings of other authors (Bhattacharya et al. 2017). The total average annual effective dose was higher in Una, Hamirpur and Kangra region recommended by UNSCEAR 2008. The annual effective dose rate (indoor and outdoor) in Siwaliks is shown in **Fig 9.**

The indoor to outdoor dose ratio observed in Siwaliks was 4.001286. A significant correlation (R^2 =0.89) was observed between the indoor to outdoor dose ratio **Fig 8.**

4.5 External and Internal Hazard Indices (H_{ex} and H_{in}):

The primary objective of external hazard index (H_{ex}) is to limit the radiation exposure due to the natural radionuclide to a permissible extent of 1 $mSvy^{-1}$.

$$H_{ex} = \frac{C_{Ra}}{370} + \frac{C_{Th}}{259} + \frac{C_K}{4810} \leq 1 \quad (11)$$

The H_{ex} in the Una, Hamirpur and Kangra region were 1.58, 2.61 and 2.55 $mSvy^{-1}$, which exceeds the standard value of unity as suggested by (ICRP 2007). The internal hazard index (H_{in}) is a radiological parameter to assess internal exposure due to carcinogenic ^{222}Rn and its decay progeny and is given by the following equation (Orgun et al. 2007)

$$H_{in} = \frac{C_{Ra}}{185} + \frac{C_{Th}}{259} + \frac{C_K}{4810} \leq 1 \quad (12)$$

The mean calculated values of H_{in} in the studied region of Una, Hamirpur and Kangra were 2.74, 4.83 and 4.69 $mSvy^{-1}$. The values of H_{ex} and H_{in} are greater than unity in all these regions and thus the soil from these localized regions is radiologically unsafe for construction purpose as per European Commission of Radiation Protection (European Commission, 1999).

4.6 Gamma level Index (I_γ):

The gamma level index (I_γ) used to estimate the γ – radiation hazard level of in the soil samples has been calculated using **Eq.(13)** given by European Commission **(**European Commission, 1999**)**.

$$I_\gamma = \frac{C_{Ra}}{300} + \frac{C_{Th}}{200} + \frac{C_K}{3000} \qquad (13)$$

The values of I_γ ranged from 0.83 to 25.01; 1.38 to 25.31 and 2.08 to 14.35 in the region of Una, Hamirpur and Kangra region respectively with an average mean value of 4.05, 6.60 and 6.41 as given in **Table 3**. The value of $I_\gamma \leq 0.5$ correspond to dose rate criterion of 0.3 mSv y^{-1}, whereas $I_\gamma \geq 0.5$ correspond to dose rate criterion of 1 mSv y^{-1}. Materials with $I_\gamma > 1.0$ should be avoided in building construction.

4.7 Excess lifetime cancer risk (ELCR)

The Excess lifetime cancer risk (ELCR) has been calculated for the assessment of extra risk of developing cancer due to exposure of a toxic substances acquired over the lifetime. ELCR has been calculated using **Eq.(14)**.

$$ELCR = AEDE \times T \times RF \qquad (14)$$

where T and RF are the duration of life (65.8 years) ((http://en.worldstat. info/Asia/India) and risk factor (0.05 Sv^{-1}) respectively. The calculated range of ELCR in Una region varied from 0.21-7.3 $x10^{-3}$, in Hamirpur it was from 0.39-7.49 $x10^{-3}$ and in Kangra, the value varied from 0.60-4.24 $x10^{-3}$. The average value of ELCR in the investigation area was higher than the world average value of 0.29×10^{-3}.

4.8 Spatial distribution of gamma dose rate

The air absorbed gamma dose measurements were carried out during the field season 2016-17. Gamma exposure rates at the sampling sites were measured by using Radiation Survey Meter (RSM). The RSM has 1" x 2" NaI(Tl) detector. The device has an energy range of 30 KeV to 3000KeV and the dose measurement range is from 1.0 μRh^{-1} to 300 mRh^{-1}. The device is calibrated using 667 keV energy of source ^{137}Cs. The air absorbed gamma dose rates D($nGyh^{-1}$) at the sampling sites in air at 1m above the ground surface for a collection time of 200 seconds for the uniform distribution of radionuclides (^{232}Th, ^{238}U and ^{40}K) were computed on the basis of guidelines provided by UNSCEAR (1993, 2000). About 5 readings are taken at a height of 1m and the arithmetic mean of the value is taken as the representative value for the gamma dose rate. These exposure rates were converted to AEDE($mSvy^{-1}$) using an outdoor occupancy factor of 0.2. Various statistical parameters like minimum, maximum and mean of AEDE values for all the three areas are shown in **Table b**. The average dose rate measured in Una is 118 $nGyh^{-1}$, while those measured in Hamirpur and Kangra are 163 $nGyh^{-1}$ and 135 nGy h^{-1} respectively. Such high dose has been estimated by Achola et al. However discrepancy is observed between the calculated and the measured dose rate (272.55, 448.93 and 407.47 nGy^{-1}) in

Una, Hamirpur and Kangra. The measurement using RSM is affected by the mineralization near the soil (around 1m from the topsoil) and radius of 10 m around its location. So the total dose rate is generated by the integration near a concentrated mineralized zone (around 1 m) and a distributed non mineralized zone (10 m). This variability in the correlation at the localized scale is counterbalanced at the global scale and a relatively low dose rate is obtained. Spatial distribution of gamma dose rate were plotted area-wise to show the variation of gamma dose rate in the given region. **(Fig 10**).

Table b Area-wise details of ambient gamma radiation measured using RSM.

Parameters	Area I (Una)	Area II (Hamirpur)	Area III (Kangra)
Min	0.027	0.14	0.12
Max	0.347	0.54	0.33
Mean	0.15	0.20	0.16

A positive correlation (R^2 = 0.63) has been observed between measured dose rate and the absorbed dose rate and the best fit is shown in **Fig 11.** A correlation between the corresponding measured dose rates and calculated dose rate has been already studied in the previous studies (Karunakaran et al., 2002; Taru et al., 2018).

With this method, it is possible to see distribution of the gamma dose rate within hundreds of kilo-metres of area. In the Una region, high gamma dose rate is observed around the Polion central location. As one moves away from this station, gamma dose start to fall off in the south as one moves towards Dadoh in the southwest. Whereas highest potassium concentration is observed in Dadoh west and lowest in Polion. The concentration of thorium is almost constant. This implies that the gamma dose rate variation is found to follow similar pattern as ^{226}Ra distribution. The ^{226}Ra concentration is similar to that of ^{238}U concentration since here the disequilibrium factor (D.F. = C_u/C_{Ra}) is in favour of daughter. The gamma dose rate at any place is correlated to the ^{226}Ra concentration at that place. Similarly in Hamirpur and Kangra the dose rate is proportional to ^{226}Ra concentration. Uranium occurs in the earth's crust either as secondary minerals or in adsorbed form and is soluble in U(VI) oxidation state and also in minerals such as zircon and monazite (Dickson and Scott, 1997). Normally thorium is immobile due to its low solubility, U, Th and K occurs in the earth as a crustal abundance of 6 ppm, 12 ppm and 1.5%. The dose rate contribution to gamma dose is primarily due to ^{238}U. The similarity of gamma dose rate to ^{226}Ra concentration can be attributed to high mineralization in this region.

4.9 Correlation studies between the individual radionuclides

A weak correlation was observed between the activity concentrations of ^{226}Ra and ^{232}Th with a correlation coefficient of r^2= 0.51. No correlation was observed between the measured radionuclides ^{232}Th and ^{40}K and ^{226}Ra and ^{232}Th (**Fig 12)** Authors have observed contrasting correlation among the radionuclides (Kovacs et al. 2013; Baeza et al. 2016, Hassan et al. 2018) however in this case it indicates that these radionuclides ^{226}Ra , ^{232}Th and ^{40}K are of different geochemical origin.

5 Conclusion

A foot based radiometric survey and soil sampling was carried out in the mineralized region of Una, Hamirpur and Kangra districts of Himachal Pradesh. The radionuclide concentration was found to be higher than the global value. The mean value of the gamma dose observed from the Una, Hamirpur and kangra district of the Siwalik region were higher when compared to the worldwide

average value as well as all Indian average value. The mean value observed is 4 times higher when compared to world average value and Indian average value.. Our data provided important information on the spatial variability of the natural terrestrial gamma radiation in the Una, Hamirpur and Kangra region. An environmental baseline gamma dose rate map of the Siwalik region over the areas of Una, Kangra and Hamirpur region is generated producing a mean value of 118 nGy h^{-1} , 163 nGyh^{-1} and 135 nGyh^{-1} which corresponds to dose rate of 0.15, 0.20 and 0.16 msv. The average dose rate was higher for grab samples since they are collected from the mineralized zones. Also a good correlation was observed between the measured gamma absorbed dose rate and the calculated gamma absorbed dose rate. The spatial dose rate map indicated the dependence of gamma dose rate on ^{238}U concentration. The data may be used for evaluating the effect of radiation on public and spatial distribution modeling may help in describing the migratory nature of radionuclides.

Acknowledgements

The author is deeply grateful to Director AMD, Dr. M.B. Verma for giving permission to complete this project

References

1. Achola, S. O., Patel, J. P., Mustapha, A. O., Angeyo, H. K., 2012. Natural radioactivity and external dose in the high background radiation area of Lambwe East, Southwestern Kenya. Radiat. Prot. Dosim. 152, 423-428. https://doi.org/10.1093/rpd/ncs047
2. Aközcan, S., Külahcı, F., Mercan, Y., 2018. A suggestion to radiological hazards characterization of ^{226}Ra, ^{232}Th, ^{40}K and ^{137}Cs: spatial distribution modeling. J. Hazard. Mater. 353, 476–489. https://doi.org/10.1016/j.jhazmat.2018.04.042
3. Al-Azmi, D., 2017. Outdoor dose rate mapping in Kuwait, J. Environ. Radioact. 169-170, 109-115. https://doi.org/10.1016/j.jenvrad.2017.01.009
4. Baeza, A., Corbacho, J. A., Guillén, J., 2016. Accuracy associated with the activity determination by in situ gamma spectrometry of naturally occurring radionuclides in soils. J. Environ. Radioact. 162-163, 219–224. https://doi.org/10.1016/j.jenvrad.2016.05.024
5. Bala, P., Mehra, R., Ramola, R.C., 2014. Distribution of natural radioactivity in soil samples and radiological hazards in building material of Una Himachal Pradesh. J. Geochem. Explor. 142, 11-15. https://doi.org/10.1016/j.gexplo.2014.02.010
6. Beretka, J., Matthew, P.J., 1985. Natural radioactivity of Australian building materials, industrial wastes and by products. Health Phys. 48, 87–95. https://doi.org/10.1097/00004032-198501000-00007
7. Bhattacharya, T., Madhavi Shankar, V., Ram Mohan Reddy, B., Thangavel, S., Sharma, P. K., 2018. Radioactivity levels in the atomic mineral occurrences along Dharmapuri Shear zone in parts of Vellore, Krishnagiri, Dharmapuri and Salem districts of Tamilnadu, India. Appl. Radiat. Isot. 132, 135-141. https://doi.org/10.1016/j.apradiso.2017.11.028
8. Bikit, I., Slivka, J., Conkic, Lj.,Krmar, M., Veskovic, M., Žikic-Todorovic, N., Varga, E., Curcic, S., Mrdja, D., 2005. Radioactivity of the soil in Vojvodina (northern province of Serbia and Montenegro). J. Environ. Radioact. 78, 11-19. https://doi.org/10.1016/j.jenvrad.2004.03.034
9. Chakraborty, A., Tripathi, R.M., Puranik, V.D., Occurences of NORM and 137Cs in soils of Singhbhum regions of eastern India and associated radiation hazard. 2009, Radioprotection 44,55-68.
10. Dickson, B.L., Scott, K.M., 1997. Interpretation of Aerial Gamma-Ray Surveys-Adding the Geochemical Factors. J. Aust. Geol. Geophys. 17, 187-200.
11. Edling, C., Comba, P., Axelson, A., Flodin, U., 1982. Effects of low-dose radiation - a correlation study. Scand. J. Work Environ. Health 8, 59-64. https://www.jstor.org/stable/40964489
12. F. Cavalcante, N.C. Silva, H.L.C. Alberti, A. De Almeida, 2011. Effective dose rate evaluation from natural gamma radiation in the region of Ribeirao Preto, SP-Brazil. Radioprotection, 46, S145–S150 DOI: 10.1051/radiopro/20116921s
13. Flodin, U., Fredriksson, M., Persson, B., Axelson, O., 1990. Acute myeloid leukemia and background radiation in an expanded case-referent study. Arch. Environ. Health 45, 364-366. https://doi.org/10.1080/00039896.1990.10118756
14. Gabdo, H. T., Ramli, A. T., Saleh, M. A., Sanusi, M. S., Garba, N. N., 2015. The influence of geology on terrestrial gamma radiation dose rate in Pahang state, Malaysia. Current Science, 109.
15. Ghiassi-nejad, M., Mortazavi, S.M., Cameron, J.R., Niroomand-rad, A., Karam, P.A., 2002. Very high background radiation areas of Ramsar, Iran: preliminary biological studies. Health Phys. 82, 87-93.

16. Grasty, R. L. and LaMarre, J. R. 2014 The annual effective dose from natural sources of ionizing radiation in Canada. Radiation Protection. Dosimetry 108, 215–226 .

17. Hassan, N. M., Kim, Y. J., Jang J., Chang B. U. and Chae J. S. 2018 Comparative study of precise measurements of natural radionuclides and radiation dose using in-situ and laboratory γ-ray spectroscopy techniques, Scientific Reports volume 8, Article number: 14115.

18. ICRP, 2007. The 2007 Recommendation of the International Commission on Radiological Protection. ICRP Publication 103.

19. International Atomic Energy Agency (IAEA). Guidelines for Radioelement Mapping Using Gamma Ray Spectrometric Data: International Atomic Energy Agency Technical Reports Series No. 1326. Austria, Vienna, (2003), p. 179.

20. Kadam, S., Chougaonkar, M.P., 2014. Assessment of ambient gamma dose rate around a prospective uranium mining area of South India - A comparativestudy of dose by direct methods and soil radioactivity measurements. Results in Phys. 4, 20-27. https://doi.org/10.1016/j.rinp.2014.02.001

21. Kardan, M.R., Fathabdi, N., Attarilar, A., Esmaeili-Gheshlaghi, M.T., Karimi, M., Najafi, A., Hosseini, S.S., 2017. A national survey of natural radionuclides in soils and terrestrial radiation exposure in Iran. J. Environ. Radioact. 178-179, 168-176. https://doi.org/10.1016/j.jenvrad.2017.08.010

22. Karunakara, N., Yashodhara I., Sudeep Kumara K., Tripathi R.M., Menon S.N., Kadam S., Chougaonkar M.P., 2014. Assessment of ambient gamma dose rate around a prospective uranium mining area of South India – A comparative study of dose by direct methods and soil radioactivity measurements. Results in Physics 4 , 20-27. https://doi.org/10.1016/j.rinp.2014.02.001.

23. Kaul, R., Khan, B.U., Khazanchi, B.M., Miglani, B.S., Mahadevan, T.M., 1979. Regional hydrogeochemical investigations for uranium in Siwalik belt of Himachal Pradesh and Punjab. Himal. Geol. 9, 773–785.

24. Kaul, R., Umamaheshwar, K., Chandrashekharan, S., Deshmukh, R. D., Swarmukar, B. M., 1993. Uranium mineralization in the Siwaliks of North Western Himalayan, India. Journal of Geol. Soc. India. 41, 243–258.

25. Kovacs, T., Szeiler, G., Fabian, F., Kardos, R., Gregoric, A., Vaupotic, J., 2013. Systematic survey of natural radioactivity of soil in Slovenia. J. Environ. Radioact. 122, 70-78. https://doi.org/10.1016/j.jenvrad.2013.02.007

26. Maharana, M., Swarnkar, M., Chougaonkar, M. P., Mayya, Y. S., Sengupta, D., 2011. Ambient gamma radiation levels (indoor and outdoor) in the villages around Jaduguda (INDIA) using card-based $CaSO_4$: Dy TL Dosemeters. Radiat. Prot. Dosim. 143, 88–96. https://doi.org/10.1093/rpd/ncq355

27. Mitas, L., Mitasova, H., 1999. Spatial Interpolation. In: Longley, P. Goodchild, M.F., Maguire, D. AndRhind, D. (eds.) Geographical Information Systems. 2nd Edition. Vol. 1: Principles and Technical Issues pp. 481-492

28. Muirhead, C.R., Butland, B.K., Green, B.M.R., Draper, G.J., 1991. Childhood leukaemia and natural radiation. Lancet 337, 503-504. https://doi.org/10.1016/0140-6736(91)93451-E

29. NazranHarun, Muhammad FathiSujan, MohdZaidi Ibrahim, 2018**.** Spatial interpolation of gamma dose in radioactive waste storage facility. IOP Conf. Series: Materials Science and Engineering **298** pp 012047 doi:10.1088/1757-899X/298/1/012047 NazranHarun*et al* 2018 *IOP Conf. Ser.: Mater. Sci. Eng.* **298** 012047

30. Organization for Economic Cooperation and Development (OECD) 1979. Exposure to radiation from the natural radioactivity in building materials. Report by a group of experts of the OECD Nuclear Energy Agency. France.

31. Örgün, Y., Altınsoy, N., Şahin, S.Y., Güngör, Y., Gültekin, A.H., Karahan, G., Karacık, Z., 2007. Natural and anthropogenic radionuclides in rocks and beach sands from Ezine region (Çanakkale), Western Anatolia, Turkey. Appl. Radiat. Isot. 65, 739-747. https://doi.org/10.1016/j.apradiso.2006.06.011

32. Patra, A. C., Sahoo, S. K., Tripathi, R. M., Puranik, V. D., 2013. Distribution of radionuclides in surface soils, Singhbhum Shear Zone, India and associated dose. Environmental Monitoring and Assessment, 185, 7833-7843. https://doi.org/10.1007/s10661-013-3138-y

33. Radhakrishna, A.P., Somashekarappa, H.M., Narayna, Y., Siddappa, K., 2003. Health Phys. 65 (1993) 390 R.I. Rudnic, S. Gao, Composition of the Continental Crust, Treatise on Geochemistry, Vol. 3, Elsevier, Amsterdam, 2003, p. 1.

34. Radiological Protection Principles Concerning the Natural Radioactivity of Building Materials. European Commission, Brussels. European Commission on Radiation Protection 112, 1999.

35. Rani, A., Singh, S., 2005. Natural radioactivity levels in soil samples from some areas of Himachal Pradesh, India using γ-ray spectrometry. Atmos. Environ. 39, 6306–6314. https://doi.org/10.1016/j.atmosenv.2005.07.050

36. Saito, K .,Jacob, P. 1995. Gamma ray fields in the air due to sources in the ground, Radiat. Prot Dosim. 58, 29-45.

37. Shacklette, H.T., Boerngen, J.G., 1984. Element Concentrations in Soils and Other Surficial Materials of the Conterminous United States.

38. Shetty, P.K., Narayana, Y., 2010. Variation of radiation level and radionuclide enrichment in high background area. J. Environ. Radioact. 30, 1–5. https://doi.org/10.1016/j.jenvrad.2010.08.003

39. Srinivas, D., Ramesh Babu, V., Patra, I., Tripathi, S., Ramayya, M.S., Chaturvedi, A.K., 2017. Assessment of background gamma radiation levels using airborne gamma ray spectrometer data over uranium deposits, Cuddapah Basin, India – A comparative study of dose rates estimated by AGRS and PGRS. J. Environ. Radioact. 167, 1-12. https://doi.org/10.1016/j.jenvrad.2016.11.027

40. Sunta, C.M., 1993; A review of the studies of high background radiation areas of the south west coast of India. In: Proceedings of the International Conference on High levels of Natural Radiation, 1990, Ramsar, Iran. IAEA Publication Series, IAEA, Vienna, 71-86.

41. Szegvary, T., Leuenberger, M. C., Conen, F., 2007. Predicting terrestrial ^{222}Rn flux using gamma dose rate as a proxy. Atmos. Chem. Phys., 7, 2789–2795.

42. United Nations Scientific Committee on the Effect of Atomic Radiation (UNSCEAR) 1988. Exposure from Natural Radiation Sources. Annex A, United Nations, New York.

43. United Nations Scientific Committee on the Effect of Atomic Radiation (UNSCEAR) 2000. Exposure due to Natural Radiation Sources. United Nations, New York.

44. United Nations Scientific Committee on the Effect of Atomic Radiation (UNSCEAR) 2008. Annexure B, United Nations, New York.

45. United Nations Scientific Committee on the Effects of Atomic Radiation (UNSCEAR) 2000 (b). Sources and effects of ionizing radiation. Report to the General Assembly with Scientific Annexes, Annex B, 104.

46. United Nations Scientific Committee on the Effects of Atomic Radiation (UNSCEAR) 1993. Report to the General Assembly, with scientific annexes. United Nations sales publication E.94.IX.2. United Nations, New York, (1993). U5 UNSCEAR. Sources and Effects of Ionizing Radiation.

47. Watson, D.F., Philip, G.M., 1985. A Refinement of Inverse Distance Weighted Interpolation. Geoprocessing, 2, 315-327.

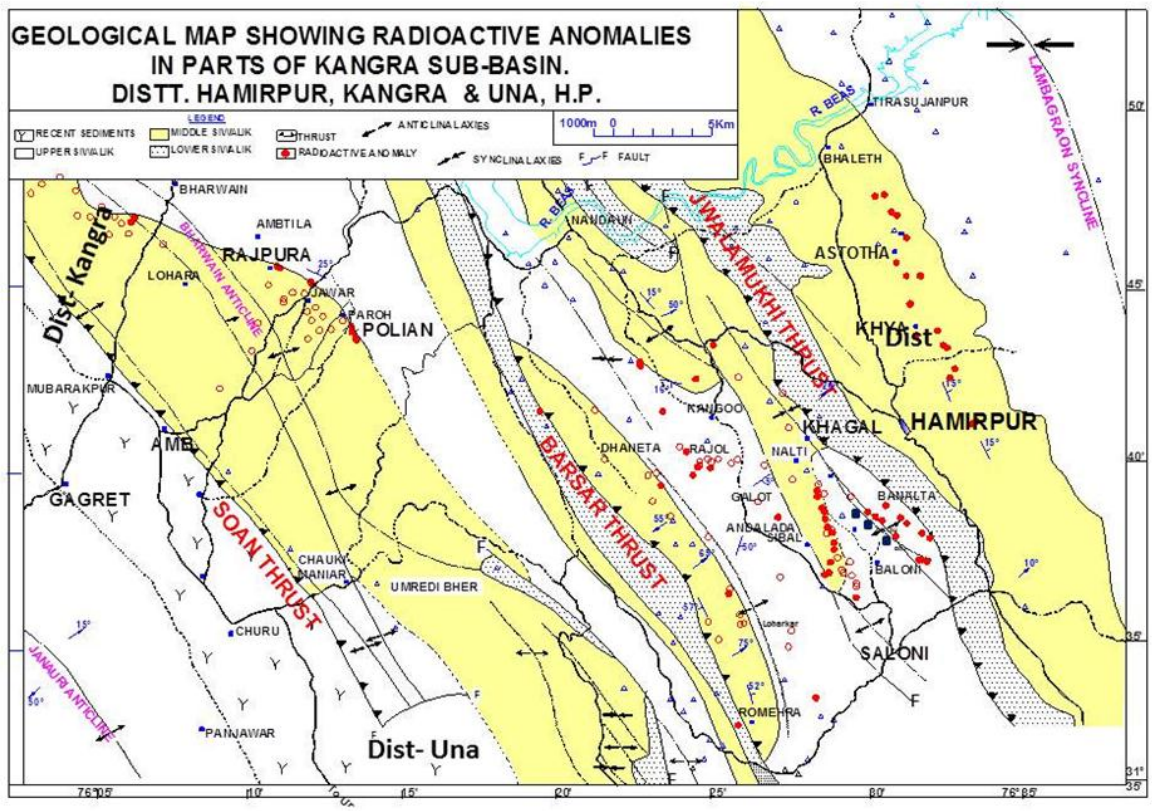

Fig. 1(a) Geological map of Siwalik region

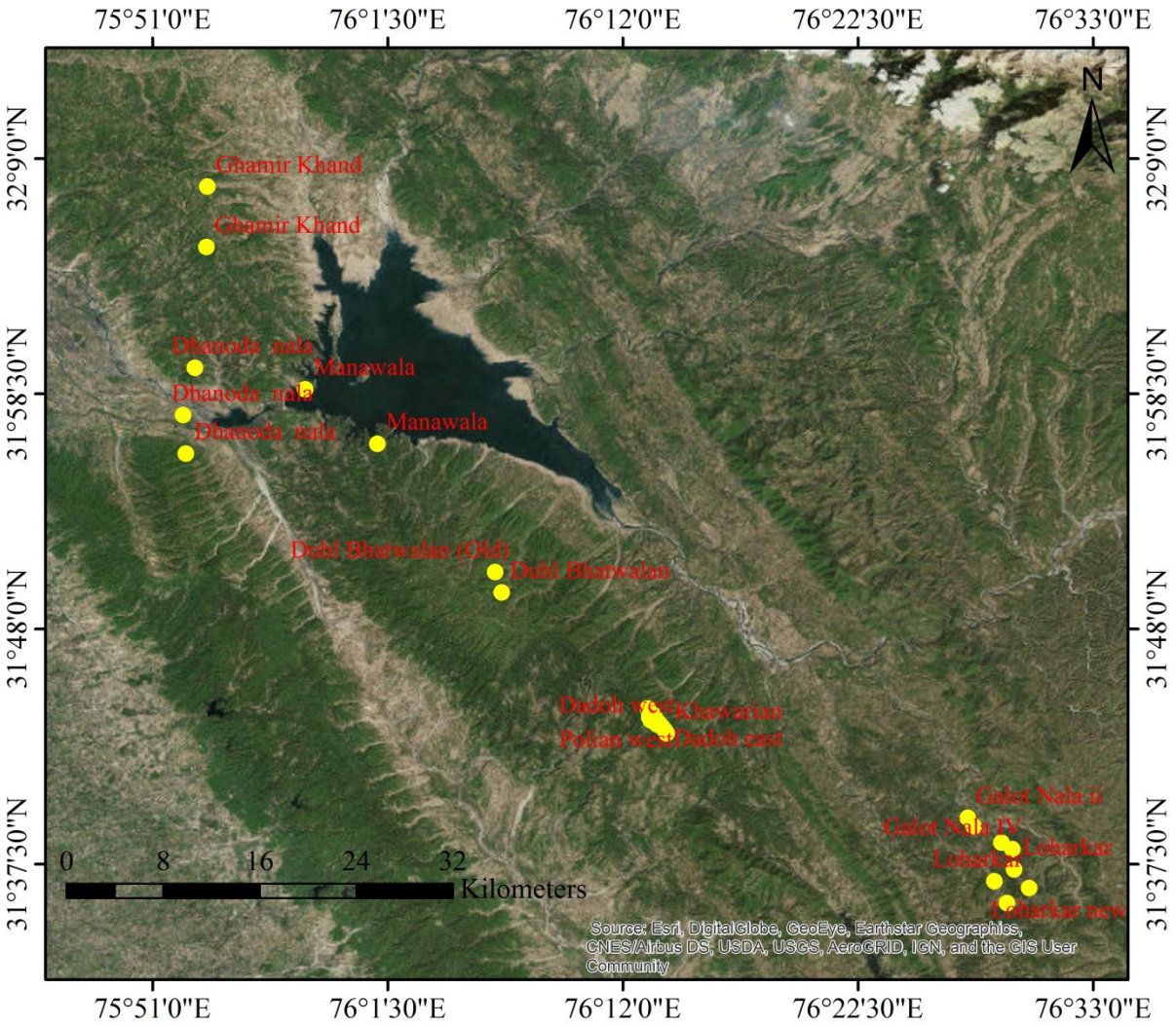

Fig. 1(b) **Sampling locations in Una, Hamirpur and Kangra region**

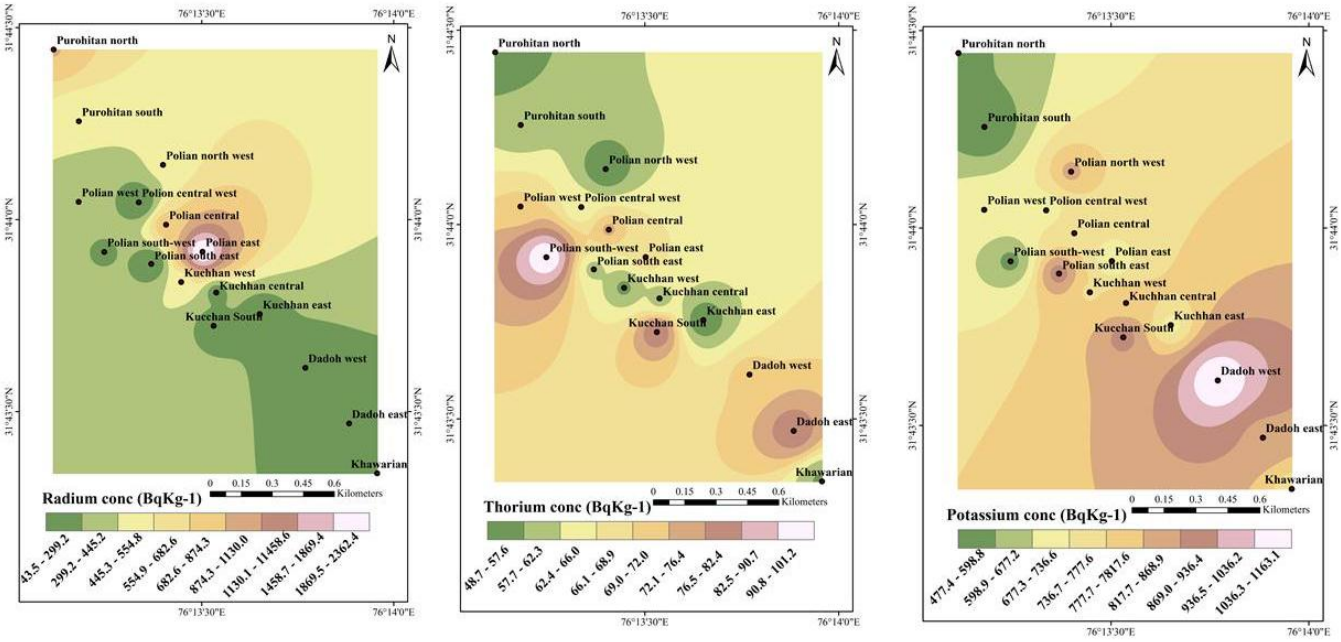

Fig. 2 Spatial activity distribution of ^{226}Ra, ^{232}Th and ^{40}K in the Una region

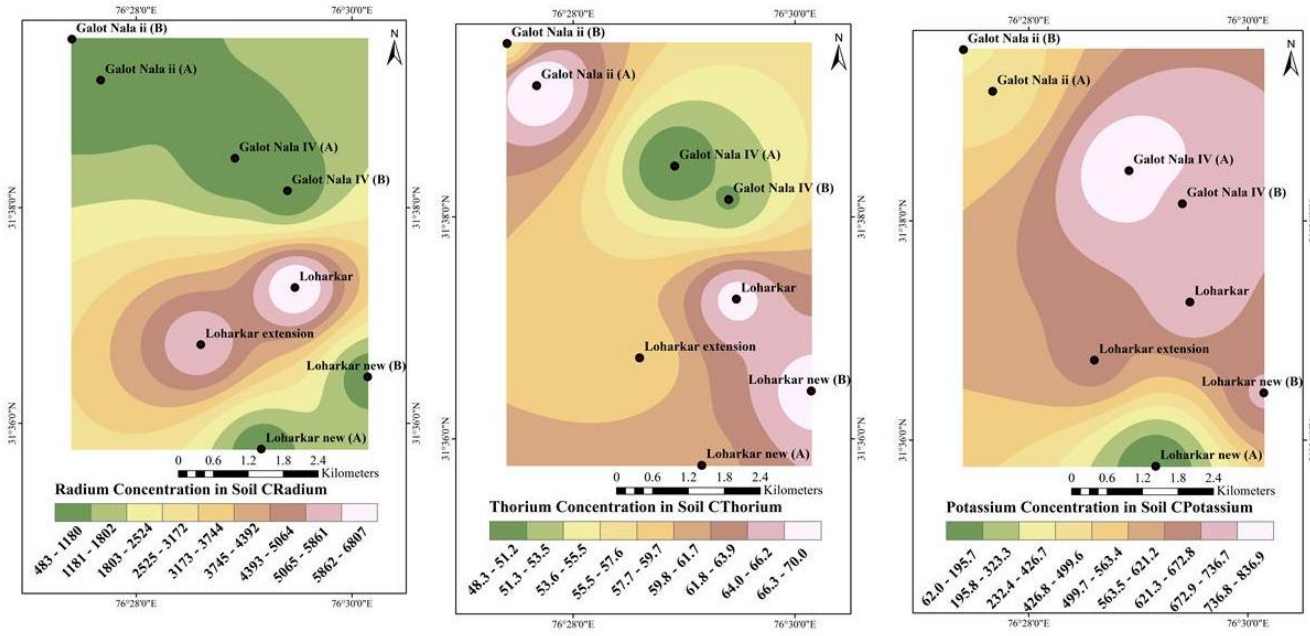

Fig. 3 Spatial activity distribution of ^{226}Ra , ^{232}Th and ^{40}K in the Hamirpur region.

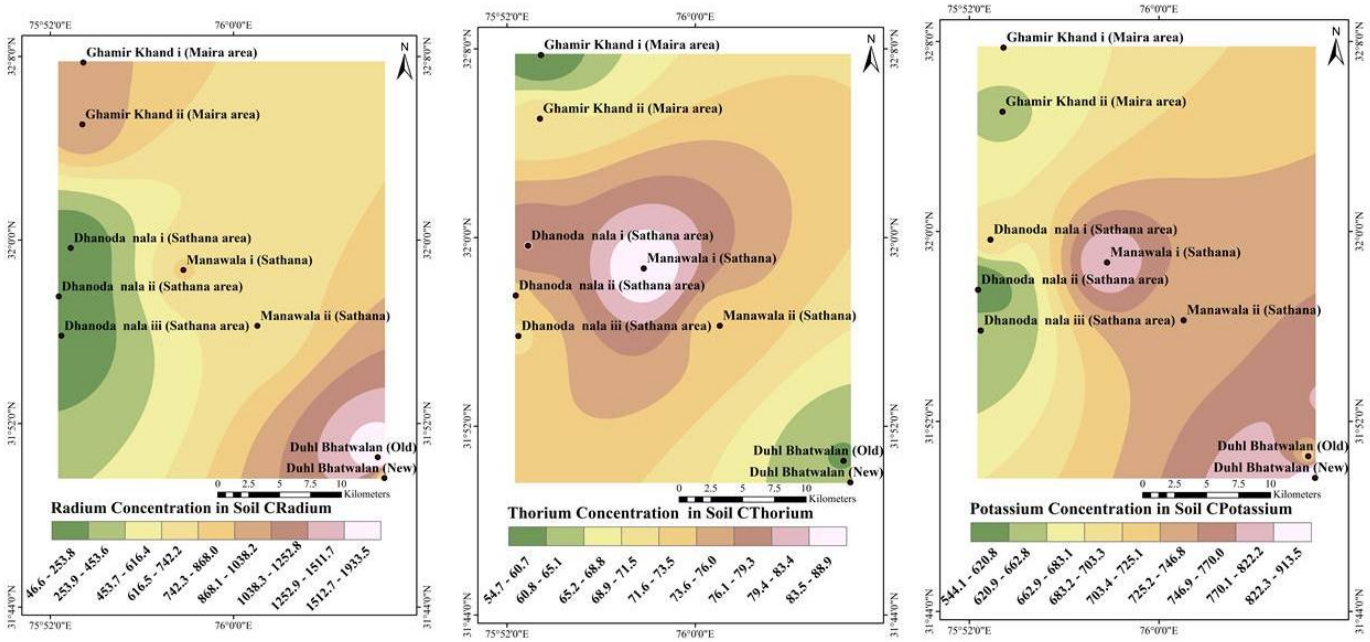

Fig. 4 Spatial activity distribution of ^{226}Ra , ^{232}Th and ^{40}K in the Kangra region.

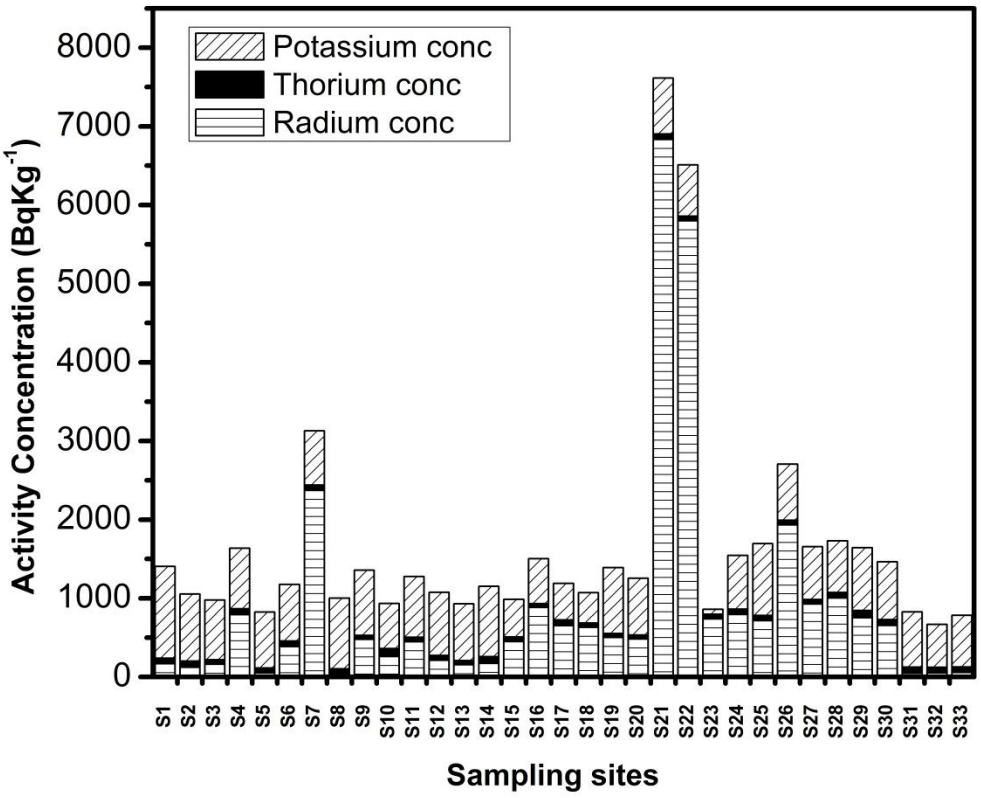

Fig: 5 Variation of the activity concentration of ^{226}Ra, ^{232}Th and ^{40}K in sampling sites.

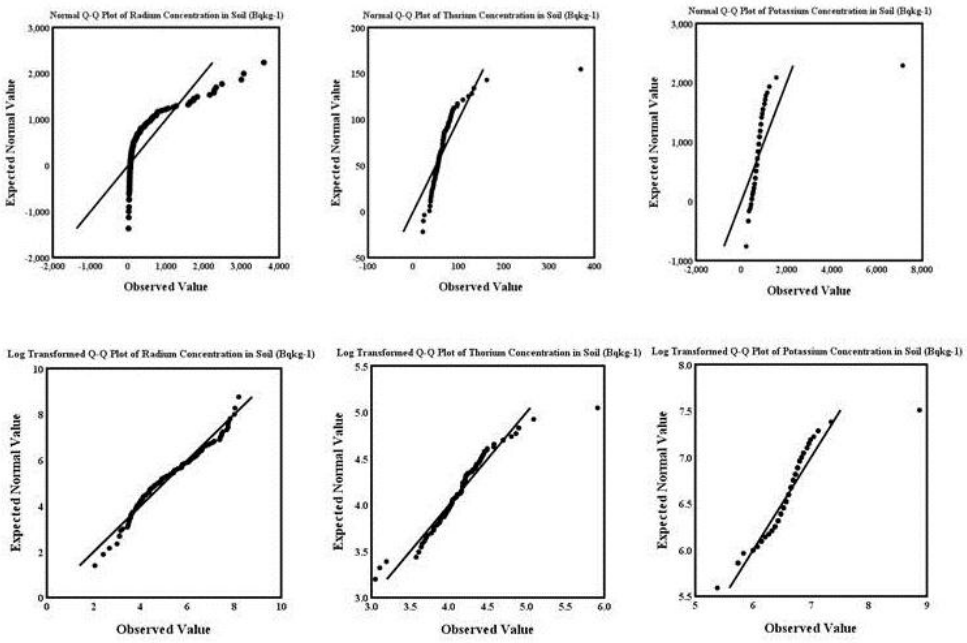

Fig: 6(a) Normal and log transformed Q-Q plots of activity concentration of ^{226}Ra, ^{232}Th and ^{40}K in Una district

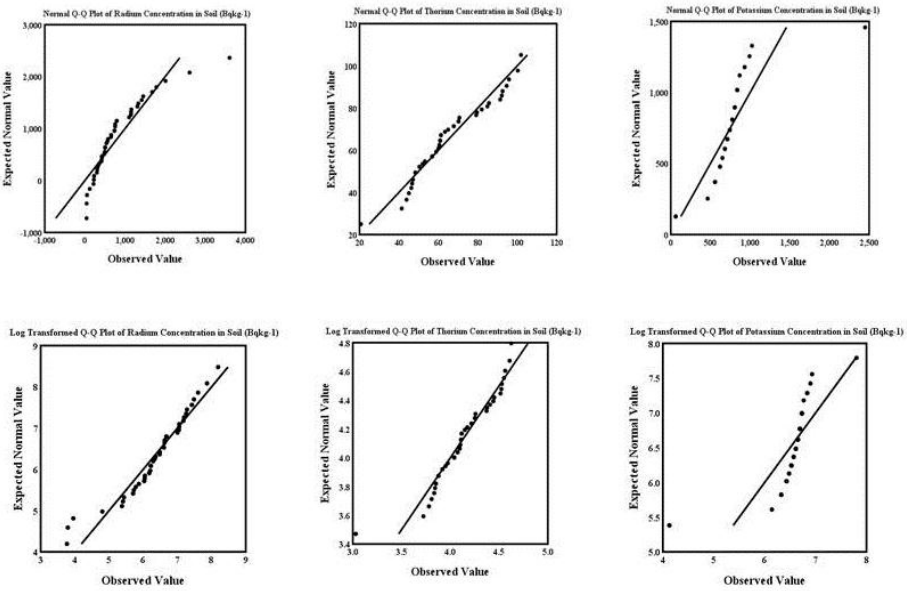

Fig: 6(b) Normal and log transformed Q-Q plots of activity concentration of ^{226}Ra, ^{232}Th and ^{40}K in Hamirpur district

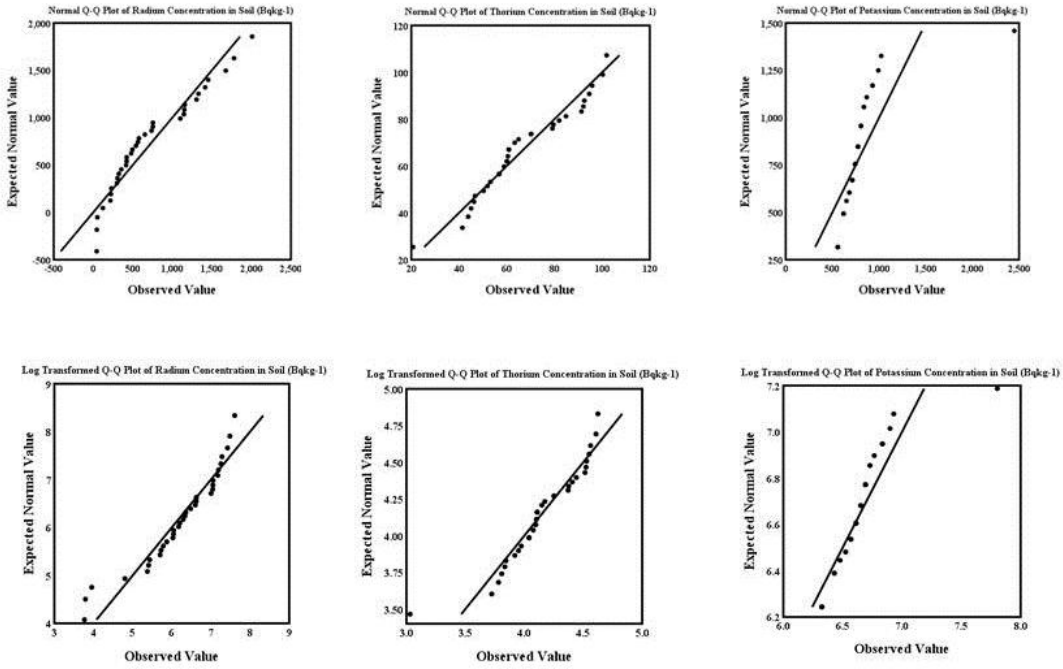

Fig: 6(c) Normal and log transformed Q-Q plots of activity concentration of ^{226}Ra, ^{232}Th and ^{40}K in Kangra district

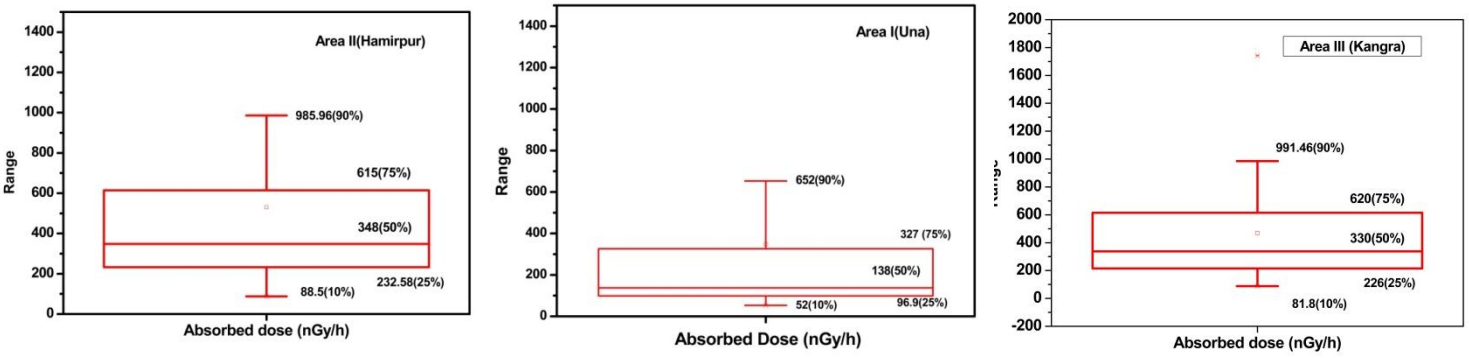

Fig: 7 Box Whisker dose rate for the air absorbed dose rate in the Una, Hamirpur and Kangra regions (No outliers were removed for the figure)

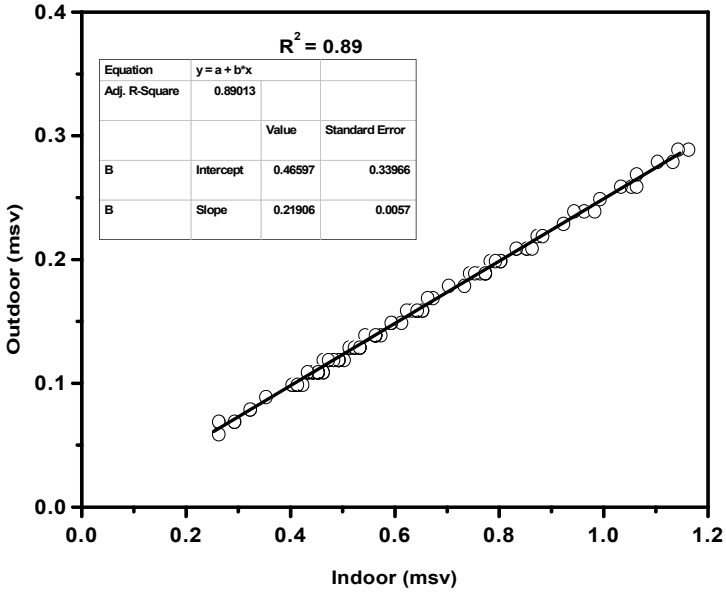

Fig: 8 Indoor to outdoor dose rate ratio in Siwalik region.

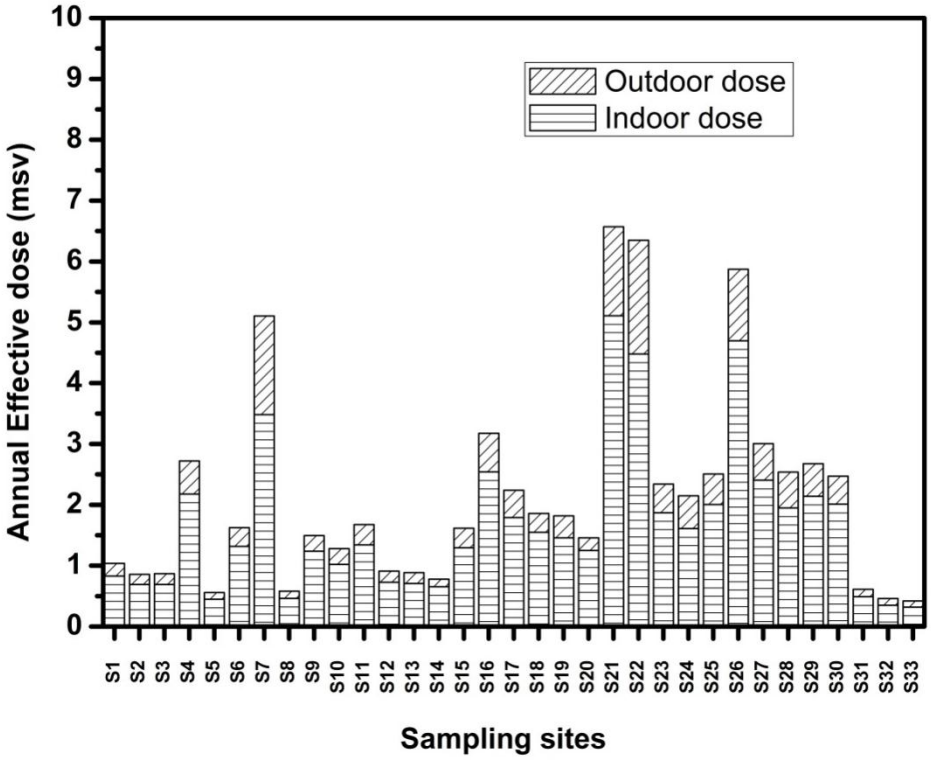

Fig. 9 Annual effective doses due to ^{226}Ra, ^{232}Th and ^{40}K

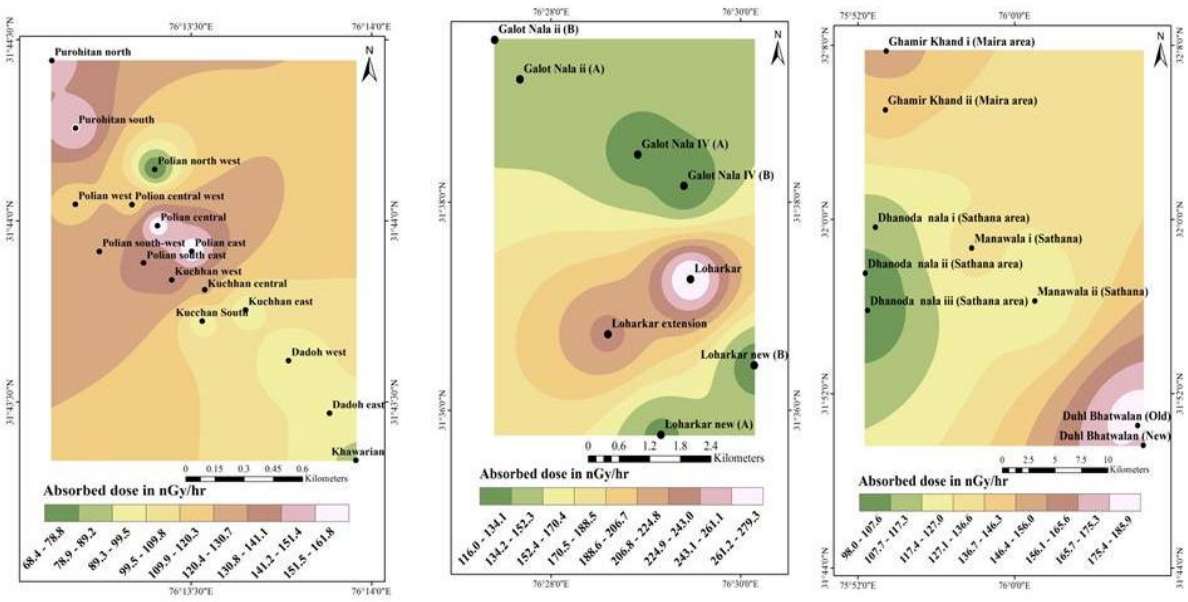

Fig. 10 Dose rate in (nGyh^{-1}) estimated from the scintillometer data over (a) Una region (b) Hamirpur region (c) Kangra region

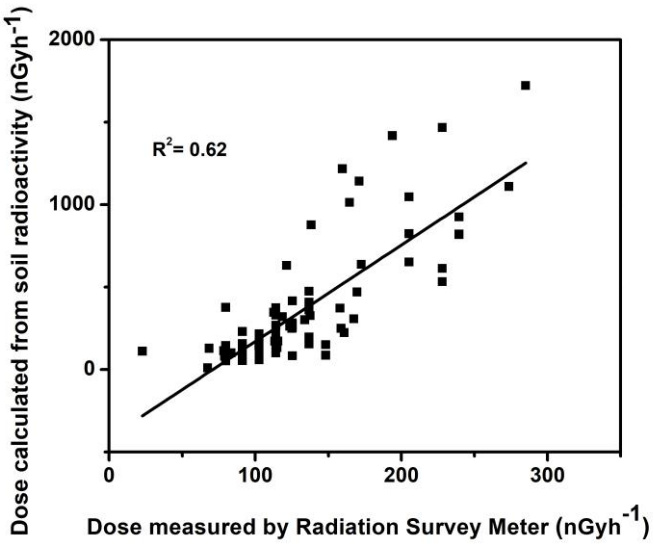

Fig. 11 Correlation between *measured* dose rate and calculated dose rate

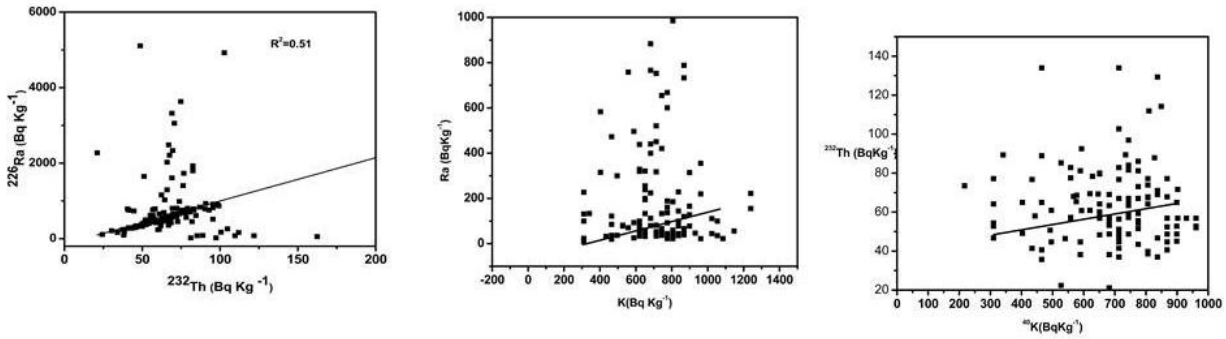

Fig. 12 Correlation between ^{226}Ra, ^{232}Th and ^{40}K radionuclides in the Siwalik region

Table 1 Details of sampling areas of Himachal Pradesh

Area No.	District	Total no. of samples	Approx. Area covered (Sq. Km.)	Area of atomic mineral occurences
1.	Una	139	20	Purohitan, Polion, Khawariyan, Kachhan, Dadoh
2.	Kangra	45	20	GhamirKhand, Manwala, Dhanotanala, DhuliBhatawan
3.	Hamirpur	34	30	Galotnala, Loharkar

Table 2. Latitude, longitude and dose rate of the sampling sites in Una, Hamirpur and Kangra districts.

Sampling Sites	Area	Latitude	Longitude	Dose rate ($nGyh^{-1}$)	Geology
S_1	Dadoh west	31° 43' 36.84" N	76° 13' 46.2" E	90	Grey Sandstone
S_2	Dadoh east	31° 43' 28.14" N	76° 13' 53.04" E	98	Grey Sandstone

S_3	Khawarian	31° 43' 20.34" N	76° 13' 57.42" E	86	Grey Sandstone
S_4	Polion Central	31° 43' 59.21" N	76° 13' 24.43" E	159	Grey Sandstone and Conglomerate mudstone
S_5	Polion Central West	31° 44' 2.69" N	76° 13' 20.17" E	116	-do-
S_6	Polion West	31° 44' 2.77" N	76° 13' 10.76" E	116	-do-
S_7	Polion East	31° 43' 54.98" N	76° 13' 30.13" E	162	-do-
S_8	Polion South East	31° 43' 53.08" N	76° 13' 22.12" E	137	Grey to buff sandstone and conglomerate and mudstone
S_9	Polion North West	31° 44' 8.55" N	76° 13' 23.94" E	68	Grey sandstone and conglomerate mudstone
S_{10}	Polion South West	31° 43' 54.95" N	76° 13' 14.76" E	125	-do-
S_{11}	Kuchhan West	31° 43' 50.24" N	76° 13' 26.79" E	135	Grey to buff sandstone and mudstone
S_{12}	Kuchhan Central	31° 43' 48.6" N	76° 13' 32.28" E	120	-do-
S_{13}	Kucchan East	31° 43' 45.24" N	76° 13' 39.06" E	93	-do-
S_{14}	Kuchhan South	31° 43' 43.39" N	76° 13' 31.87" E	91	-do-
S_{15}	Purohitan South	31° 44' 15.36" N	76° 13' 10.8" E	145	Grey to buff sandstone and conglomerate and mudstone
S_{16}	Purohitan North	31° 44' 26.58" N	76° 13' 6.84" E	152	-do-
S_{17}	GalotNala II(A)	31° 39' 33.69" N	76° 27' 24.28" E	145	Grey coloued fine grained sandstone with pebbles
S_{18}	GalotNala II(B)	31° 39' 10.91" N	76° 27' 40.3" E	140	-do-
S_{19}	GalotNala IV(A)	31° 38' 9.39" N	76° 29' 24.19" E	125	Grey coloured sandstone with pebbles
S_{20}	GalotNala IV(B)	31° 38' 27.46" N	76° 28' 54.96" E	116	-do-
S_{21}	Loharkar old	31° 37' 15.52" N	76° 29' 28.35" E	280	Coarse grained red colour oxidized sandstone
S_{22}	Loharkar extensiom	31° 36' 43.74" N	76° 28' 36.01" E	230	-do-
S_{23}	Loharkar new (A)	31° 35' 45.65" N	76° 29' 9.61" E	130	Coarsed grained reddish sandstone
S_{24}	Loharkar new (B)	31° 36' 25.82" N	76° 30' 8.8" E	125	-do-
S_{25}	DhuliBhatawan new	31° 49' 37.42" N	76° 6' 35.23" E	170	Light grey sandstone
S_{26}	DhuliBhatawan old	31° 50' 31.95" N	76° 6' 17.91" E	185	Coarse sandstone with fresh feldspar
S_{27}	GhamirKhand(i) Maira area	32° 7' 44.41" N	75° 53' 26.71" E	154	Grey coloured medium grained Micaceous sandstone
S_{28}	GhamirKhand (ii) Maira area	32° 5' 2.51" N	75° 53' 24.14" E	140	Grey coloured sandstone with clay
S_{29}	Manawala (i) (Sathana)	31° 58' 41.69" N	75° 57' 48.8" E	130	Grey colour siltstone with clay patches

S_{30}	Manawala (ii) (Sathana)	31° 59' 30.5" N	525 ± 57	120	Drak grey coloured shale
S_{31}	DhanotaNala (i)	31° 57' 32.35" N	75° 52' 22.34" E	115	Light grey very coarse grained sandstone
S_{32}	DhanotaNala(ii)	31° 55' 49.56" N	75° 52' 29.19" E	98	Fine grained light sandstone
S_{33}	DhanotaNala (iii)	31° 56' 23.5" N	75° 51' 10.5" E	100	Light grey sandstone

Table 3 Descriptive statistics of radiological concentration and radiological hazard indices in each sampling location (n=218).

parameter	Region	Mean	Median	GM	Variance	S.D	Min	Max	Range (R)	Inter Quartile	Sk	K	MAD
Ra ($Bqkg^{-1}$)	Una	432.98	129.31	160.06	478825.02	691.97	7.77	3593.07	3585.30	415.80	2.48	6.10	465.14
	Hamirpur	818.22	614.94	564.52	495653.61	704.02	43.29	3603.06	3559.77	779.75	1.96	5.08	504.69
	Kangra	789.10	577.22	629.13	272143.2	521.87	121.89	2009.10	1887.21	769.23	0.821	-0.37	436.64
Th ($Bqkg^{-1}$)	Una	66.30	62.11	61.68	1149.30	33.90	21.11	369.94	348.83	21.86	5.71	47.85	17.57
	Hamirpur	65.04	60.90	62.39	334.09	18.27	20.70	101.90	81.20	28.72	0.30	-0.25	14.58
	Kangra	66.80	60.90	64.57	320.46	17.90	41.41	100.20	58.87	30.85	0.492	-1.02	115.06
K ($Bqkg^{-1}$)	Una	764.29	713.00	698.53	342648.16	585.36	217	7130	6913	217.00	9.65	105.31	697.98
	Hamirpur	753.86	744.00	676.08	103017.98	320.96	62	2499	2387	186.00	3.09	18.80	159.67
	Kangra	814.55	744.00	779.04	111606.18	334.07	558	2449	1891	140.00	4.43	22.07	154.07
Ra_{eq} ($Bqkg^{-1}$)	Una	581.30	281.48	378.15	479275.46	692.29	110.59	3725.12	3614.53	431.83	2.45	5.86	464.28
	Hamirpur	964.01	768.08	773.66	495241.69	703.73	179.93	3771.33	3591.20	799.11	1.98	5.23	505.85
	Kangra	941.66	747.70	812.57	268915.74	518.57	278.42	2126.05	1847	796.82	0.77	-0.49	435.10
D ($nGyh^{-1}$)	Una	272.55	133.06	179.87	101855.61	319.14	52.67	1722.38	1669.71	198.60	2.45	5.84	214.64
	Hamirpur	448.93	356.67	334.57	105235.58	324.40	87.96	1741.33	1653.37	371.40	1.98	5.21	233.41
	Kangra	407.47	384.17	380.37	57200.39	239.16	135.20	985.60	850.64	368.60	0.77	-0.49	200.69
AEDE Indoor ($mSvy^{-1}$)	Una	1.33	0.65	0.88	2.45	1.56	0.26	8.45	8.19	0.97	2.45	5.85	1.04
	Hamirpur	2.20	1.75	1.77	2.53	1.59	0.43	8.54	8.11	1.82	1.98	5.21	1.14
	Kangra	2.15	1.71	1.86	1.33	1.17	0.66	4.38	4.17	1.80	0.77	-0.49	0.98
AEDE Outdoor ($mSvy^{-1}$)	Una	0.33	0.16	0.22	0.15	0.39	0.06	2.11	2.05	0.23	2.45	5.86	0.26
	Hamirpur	0.55	0.44	0.44	0.16	0.39	0.11	2.14	2.03	0.45	1.99	5.27	0.28
	Kangra	0.53	0.43	0.46	0.086	0.29	0.17	1.21	1.04	0.45	0.78	-0.47	0.24
H_{in}	Una	2.74	1.09	1.52	13.99	3.74	0.25	19.79	19.44	2.19	2.47	5.97	2.50

	Hamirpur	4.80	3.73	3.68	3.80	14.46	0.62	19.94	19.32	4.37	1.97	5.16	2.73
	Kangra	4.69	3.56	3.92	7.89	2.80	1.10	11.19	10.09	4.29	0.79	-0.49	2.35
H_{ex}	Una	1.58	0.77	1.03	3.50	1.87	0.31	10.08	9.77	1.16	2.45	5.85	1.25
	Hamirpur	2.61	2.08	2.11	3.62	1.90	0.50	10.20	9.70	2.17	1.98	5.22	1.36
	Kangra	2.55	2.03	2.21	1.96	1.40	0.77	5.76	4.99	2.16	0.77	-0.43	1.17
$I\gamma$	Una	4.05	2.05	2.74	13.99	3.74	0.83	25.01	24.18	2.85	2.44	5.81	3.10
	Hamirpur	6.60	5.28	5.38	22.01	4.69	1.38	25.31	23.93	5.36	1.98	5.22	3.37
	Kangra	6.47	5.18	5.63	11.95	3.45	2.08	14.35	12.27	5.34	0.76	-0.50	2.90
ECLR	Una	1.17	0.56	0.77	1.87	1.36	0.21	7.39	7.18	0.83	2.45	5.36	0.91
	Hamirpur	1.93	1.54	1.56	1.93	1.39	0.39	7.49	7.10	1.58	1.99	5.26	1.00
	Kangra	1.88	1.56	1.64	1.01	1.00	0.60	4.24	3.64	1.56	0.80	-0.36	0.83

Table 4. Comparison of Dose rate with other atomic mineral occurence and HLNRA areas of India and world

Locations	Dose rate			References
	Min	Max	Average	
LambweEast,Kenya	0.7 µGyh^{-1}	6.0 µGyh^{-1}	2.3µGyh^{-1}	Achola et al., 2002
Dharmapuri, Tamilnadu	0.02µGyh^{-1}	3.26 µGyh^{-1}	0.35µGyh^{-1}	Taru et al., 2018
Jaduguda,	696 µGyy^{-1}	1223µGyy^{-1}	959.5	Maharana et al., 2011
West Antolia, Turkey	-	-	527.9 nGyh^{-1}	Orgen et al., 2007
Neendkara, Kerala	1475 nGyh^{-1}	28,388 nGyh^{-1}	9795 nGyh^{-1}	Derin et al. ,2012
Erasama, Orissa	650 nGyh^{-1}	3150 nGyh^{-1}	1925 nGyh^{-1}	Mohanty et al. 2004
Singhbhum	59 nGyh^{-1}	900 nGyh^{-1}	99nGyh^{-1}	Patraet al., 2013
Quilon, kerala	43 nGyh^{-1}	17,400 nGyh^{-1}	5709 nGyh^{-1}	Shetty et al., 2010
Siwaliks	87.96 nGyh^{-1}	1741.33 nGyh^{-1}	448.23 nGyh^{-1}	Present Study